MOLECULAR AND CELLULAR BIOLOGY, Jan. 2009, p. 503–514 Vol. 29, No. 2
0270-7306/09/$08.00+0 doi:10.1128/MCB.01354-08

Artemis and Nonhomologous End Joining-Independent Influence of DNA-Dependent Protein Kinase Catalytic Subunit on Chromosome Stability▽†

Travis H. Stracker,[1] Bret R. Williams,[2]‡ Ludovic Deriano,[3] Jan W. Theunissen,[1]§ Carrie A. Adelman,[1] David B. Roth,[3] and John H. J. Petrini[1]*

Molecular Biology Program, Sloan-Kettering Institute, Memorial Sloan-Kettering Cancer Center and Cornell University Graduate School of Medical Sciences, New York, New York 10065[1]; Laboratory of Genetics, University of Wisconsin Medical School, Madison, Wisconsin 53705[2]; and Kimmel Center for Biology and Medicine of the Skirball Institute and Department of Pathology, New York University School of Medicine, New York, New York 10016[3]

Received 25 August 2008/Returned for modification 16 September 2008/Accepted 6 November 2008

Deficiency in both ATM and the DNA-dependent protein kinase catalytic subunit (DNA-PKcs) is synthetically lethal in developing mouse embryos. Using mice that phenocopy diverse aspects of *Atm* deficiency, we have analyzed the genetic requirements for embryonic lethality in the absence of functional DNA-PKcs. Similar to the loss of ATM, hypomorphic mutations of Mre11 (*Mre11*^{ATLD1}) led to synthetic lethality when juxtaposed with DNA-PKcs deficiency (*Prkdc*^{scid}). In contrast, the more moderate DNA double-strand break response defects associated with the *Nbs1*$^{\Delta B}$ allele permitted viability of some *Nbs1*$^{\Delta B/\Delta B}$ *Prkdc*$^{scid/scid}$ embryos. Cell cultures from *Nbs1*$^{\Delta B/\Delta B}$ *Prkdc*$^{scid/scid}$ embryos displayed severe defects, including premature senescence, mitotic aberrations, sensitivity to ionizing radiation, altered checkpoint responses, and increased chromosome instability. The known functions of DNA-PKcs in the regulation of Artemis nuclease activity or nonhomologous end joining-mediated repair do not appear to underlie the severe genetic interaction. Our results reveal a role for DNA-PKcs in the maintenance of S/G_2-phase chromosome stability and in the induction of cell cycle checkpoint responses.

The Mre11 complex, consisting of Mre11, Rad50, and Nbs1 (Xrs2 in *Saccharomyces cerevisiae*), is involved in diverse aspects of DNA double-strand break (DSB) metabolism. The Mre11 complex acts as a DSB sensor, mediates cell cycle checkpoint arrest and apoptosis, and promotes DSB repair (47, 48). The influence of the Mre11 complex on DSB responses is attributable partly to its influence on ataxia-telangiectasia mutated (ATM) kinase activity (29). ATM is a central signal transducer in the response to DSBs and is required for arrest throughout the cell cycle, as well as the efficient execution of apoptosis in response to many types of genotoxic stress (43).

The Mre11 complex is required for ATM activation and governs the phosphorylation of ATM substrates such as SMC1, Chk2, and BID (4, 6, 26, 47, 49, 51). The C terminus of Nbs1 interacts with ATM and plays an important role in facilitating a subset of these events, particularly those important for apoptosis (11, 14, 47, 58). However, ATM makes multiple functional contacts with members of the Mre11 complex. Nbs1, Mre11, and Rad50 are all ATM substrates, and many aspects of ATM checkpoint signaling are impaired by hypomorphic *Mre11* and *Nbs1* mutations that do not affect the ATM binding domain in the C terminus of Nbs1 (32, 36, 52, 54).

Several molecular and genetic observations support the view that the Mre11 complex's role in preserving genome stability is particularly relevant to the S and G_2 phases of the cell cycle (3, 56). The complex, predominantly nucleoplasmic in G_1 cells, becomes predominantly chromatin associated and colocalizes with PCNA throughout S phase (35, 38). This association is a likely prerequisite for the complex's influence on DNA damage signaling as well as DNA repair.

Cell cultures established with samples from patients with Nijmegen breakage syndrome (*NBS1* hypomorphism) and ataxia-telangiectasia-like disorder (*MRE11* hypomorphism) exhibit checkpoint defects in S phase and at the G_2/M transition, while the G_1/S transition is relatively unaffected. These checkpoint defects are correlated with reduced Mre11 complex chromatin association both in human cells and in mouse models of Nijmegen breakage syndrome and ataxia-telangiectasia-like disorder (5, 45, 49, 52). Chromosomal aberrations arising in these cells are predominantly chromatid type breaks, consistent with impaired metabolism of DNA replication-associated DNA breaks (49, 52).

Further supporting a predominant role for the Mre11 complex in S phase is the observation that its primary role in DSB repair is the promotion of recombination between sister chromatids (3, 24). Structural and genetic evidence that the Mre11 complex effects molecular bridging between DNA duplexes offers a mechanistic basis for this observation (10, 23, 53). Molecular bridging by the Mre11 complex may also contribute

* Corresponding author. Mailing address: Molecular Biology Program, Sloan-Kettering Institute, Memorial Sloan-Kettering Cancer Center and Cornell University Graduate School of Medical Sciences, New York, NY 10065. Phone: (212) 639-2927. Fax: (646) 422-2062. E-mail: petrinij@mskcc.org.

† Supplemental material for this article may be found at http://mcb.asm.org/.

‡ Present address: David H. Koch Institute for Integrative Cancer Research, Howard Hughes Medical Institute, Massachusetts Institute of Technology, Cambridge, MA 02142.

§ Present address: Nature Biotechnology, 75 Varick St., 9th Floor, New York, NY 10013.

▽ Published ahead of print on 17 November 2008.

to its influence on nonhomologous end joining (NHEJ) (12, 34, 57). Collectively, these data strongly support the view that the Mre11 complex's checkpoint and DSB repair functions are manifested predominantly in the S and G_2 phases of the cell cycle.

Although the Mre11 complex and ATM function in the same arm of the DNA damage response, ATM deficiency is lethal in hypomorphic *Mre11* and *Nbs1* mutants ($Mre11^{ATLD1/ATLD1}$ and $Nbs1^{\Delta B/\Delta B}$ mice, respectively) (49, 52), suggesting that aspects of ATM function are Mre11 complex independent. ATM deficiency is also synthetically lethal with mutations in *Prkdc*, the gene encoding the catalytic subunit of the DNA-dependent protein kinase (DNA-PKcs) that is mutated in mice with severe combined immunodeficiency ($Prkdc^{scid}$ mice) (22, 42). DNA-PKcs is an ATM paralog required for NHEJ, which appears to be the predominant mode of DSB repair in G_1 cells (16).

Defective NHEJ is unlikely to be the basis for the embryonic lethality of $Prkdc^{-/-}$ $Atm^{-/-}$ or $Prkdc^{scid/scid}$ $Atm^{-/-}$ mice, as loss of ATM rescues the late embryonic lethality of both DNA ligase IV (*Lig4*) and *XRCC4* null embryos, which have more severe NHEJ defects than $Prkdc^{scid}$ mice abolished by the $Atm^{-/-}$ genotype (31, 42). These observations argue that the DNA-PKcs functions required for viability in the absence of ATM do not include NHEJ.

To address this issue, we crossed $Mre11^{ATLD1/ATLD1}$ and $Nbs1^{\Delta B/\Delta B}$ mice with $Prkdc^{scid/scid}$ mice. As these Mre11 complex hypomorphs do not completely phenocopy ATM deficiency, we reasoned that double-mutant animals would be viable and thus provide a venue in which to examine the functional relationship between the Mre11 complex/ATM arm of the DNA damage response and DNA-PKcs. Whereas the $Mre11^{ATLD1/ATLD1}$ mutation was synthetically lethal with the $Prkdc^{scid/scid}$ genotype, some $Nbs1^{\Delta B/\Delta B}$ $Prkdc^{scid/scid}$ mice were born, consistent with the more moderate DNA damage response defects associated with the $Nbs1^{\Delta B}$ allele than with the $Mre11^{ATLD1}$ allele (48). $Nbs1^{\Delta B/\Delta B}$ $Prkdc^{scid/scid}$ embryos were born at drastically reduced Mendelian ratios, displayed gross developmental defects, and were severely runted. $Nbs1^{\Delta B/\Delta B}$ $Prkdc^{scid/scid}$ cell cultures exhibited profound chromosome instability, growth defects, and increased sensitivity to ionizing radiation (IR). DNA repair defects associated with DNA-PKcs deficiency did not appear to underlie the observed phenotypic synergy. Rather, the data suggest a novel regulatory function of DNA-PKcs in the maintenance of chromosomal stability during the S and G_2 phases of the cell cycle.

MATERIALS AND METHODS

Mice and genotyping. $Mre11^{ATLD1/ATLD1}$ and $Nbs1^{\Delta B/\Delta B}$ mice were generated as described previously (49, 52). $Atm^{-/-}$ mice were obtained from T. Wynshaw Boris, $Smc1^{2SA/2SA}$ mice were obtained from M. Kastan, and $Art^{-/-}$ mice were obtained from F. Alt. $Prkdc^{scid/scid}$ mice were purchased from the Jackson Laboratory. All mice were maintained on a mixed 129SvEv/C57B6 background and genotyped by PCR (details are available upon request).

Antibodies, Western blotting, and immunofluorescence. Antibodies for Nbs1 were described previously (52). Antibodies for Myc (Sloan-Kettering Institute Monoclonal Antibody Core Facility) and actin (Sigma) were purchased. Cell extracts were prepared in 150 mM TNG buffer (50 mM Tris, pH 7.5, 150 mM NaCl, 1% Tween 20, 0.5% NP-40), run on sodium dodecyl sulfate-polyacrylamide gel electrophoresis gels, and transferred onto a polyvinylidene difluoride membrane (Millipore). Primary and secondary antibodies were incubated with the membrane in 5% dry milk in phosphate-buffered saline (PBS) with 0.05% Tween 20, and antibody detection was performed using enhanced chemiluminescence with a kit from GE Healthcare.

MEF derivation and culture. Primary and transformed mouse embryonic fibroblasts (MEFs) were generated from appropriate crosses as described previously (50). For proliferation assays, passage 1 (p1) MEFs were seeded at 5×10^5 per well onto a six-well plate. Cells were trypsinized and counted every 3 days for a total of 12 days. Total proliferation was determined by calculating the number of cells that would have been recovered had all cells been replated at every counting.

Chromosome analysis and telomere fluorescence in situ hybridization (FISH). For mitotic analysis, early-passage (p2 to p3) MEFs were grown on sterile microscope slides, fixed in PBS containing 4% paraformaldehyde and 2% sucrose, and permeabilized in a solution of 10 mM HEPES, pH 7.9, 50 mM NaCl, 3 mM $MgCl_2$, 200 mM sucrose, and 0.5% Triton X-100. Cells were stained with DAPI (4′,6-diamidino-2-phenylindole), mounted in Prolong Antifade reagent (Molecular Probes), and scored for abnormalities.

For metaphase analysis, early-passage (p2 to p5) or simian virus 40 (SV40)-transformed ear fibroblasts (EFs) or MEFs were prepared as described previously (50). Metaphase spreads were treated with Giemsa stain (Sigma) and mounted in Permount. For fusion analysis, telomere FISH was performed as described previously (28) using a fluorescein isothiocyanate-conjugated peptide nucleic acid probe (fluorescein isothiocyanate-5′-CCCTAACCCTAACCCTAA-3′; Applied Biosystems).

DNA damage sensitivity assays and checkpoint analysis. IR sensitivity assays were performed as described previously (50). Exponentially growing SV40-transformed MEFs were treated with mitomycin C (MMC; Sigma) for 2 h or with camptothecin (CPT; Sigma) for 24 h, washed twice with PBS, and analyzed for colony formation. Plates were stained with crystal violet, and colonies with more than 50 cells were counted. The numbers of colonies growing on plates that received treatment were normalized to the numbers on mock-treated plates. Intra-S-phase, G_1/S, and G_2/M checkpoint assays were performed as described previously (50).

Viral infection. Plasmid containing the dominant negative $Trf2^{\Delta B\Delta M}$ allele was a gift from T. de Lange. Adenovirus expressing green fluorescent protein (Ad-GFP) and adenovirus expressing $Trf2^{\Delta B\Delta M}$ were purchased from the University of Iowa Gene Transfer Vector Core. MEFs were infected with adenovirus vectors at a multiplicity of infection of 100 for 16 h, after which time the cells were washed and cultured in fresh medium. Metaphase spreads for fusion analysis were prepared 40 h postinfection.

Statistical analysis. Statistical analysis was performed using MStat software (provided by Norman Drinkwater, McArdle Laboratory for Cancer Research) or Excel (Microsoft).

RESULTS

Genetic analysis of synthetic lethality. ATM influences DSB responses throughout the cell cycle, whereas defects in hypomorphic Mre11 complex mutants are restricted to the S and G_2 phases. To determine if defects in S- and G_2-phase DSB responses interacted genetically with *Prkdc* deficiency, we established intercrosses to generate $Mre11^{ATLD1/ATLD1}$ $Prkdc^{scid/scid}$ and $Nbs1^{\Delta B/\Delta B}$ $Prkdc^{scid/scid}$ double mutants. No viable $Mre11^{ATLD1/ATLD1}$ $Prkdc^{scid/scid}$ embryos were recovered, indicating synthetic lethality between $Mre11^{ATLD1}$ and $Prkdc^{scid}$ (Table 1). Expected genotypic ratios were observed at embryonic day 3.5 (E3.5) and E10.5, but by E10.5, all double-mutant embryos were runted, displayed abnormal morphology, or were partially reabsorbed, and attempts to culture cells from these embryos were not successful (Table 1 and data not shown).

Embryonic lethality was also observed in $Nbs1^{\Delta B/\Delta B}$ $Prkdc^{scid/scid}$ mutants, but unlike the lethality of the $Mre11^{ATLD1/ATLD1}$ $Prkdc^{scid/scid}$ genotype, this outcome was not fully penetrant, and double-mutant animals were born at about 5% of the expected frequency. Developmental defects were evident in double-mutant $Nbs1^{\Delta B/\Delta B}$ $Prkdc^{scid/scid}$ embryos (Fig. 1A and B and data not shown; see also Table S1 in the supplemental

TABLE 1. *Mre11*$^{ATLD1/ATLD1}$ *Prkdc*$^{scid/scid}$ mutant data

Genotype of father	Genotype of mother	Time point of assessment	Total no. of embryos	Total no. of pups	Expected no. of double mutants	Observed no. of double mutants	*P* value[b]
Mre11$^{+/ATLD1}$ *Prkdc*$^{scid/scid}$	*Mre11*$^{+/ATLD1}$ *Prkdc*$^{scid/scid}$	E10.5	15		3.75	3[a]	
		E3.5	10		2.5	3	
Mre11$^{+/ATLD1}$ *Prkdc*$^{+/scid}$	*Mre11*$^{+/ATLD1}$ *Prkdc*$^{+/scid}$	After birth		203	12.7	0	2.0×10^{-6}
Mre11$^{+/ATLD1}$ *Prkdc*$^{scid/scid}$	*Mre11*$^{+/ATLD1}$ *Prkdc*$^{+/scid}$	After birth		35	4.4	0	9.4×10^{-3}
Mre11$^{+/ATLD1}$ *Prkdc*$^{scid/scid}$	*Mre11*$^{+/ATLD1}$ *Prkdc*$^{scid/scid}$	After birth		62	15.5	0	1.8×10^{-8}

[a] Embryos were partially reabsorbed or were abnormal or runted.
[b] *P* values are based on binomial distribution.

material), and the rare double-mutant pups that survived to term were severely runted (Fig. 1B).

The observed phenotypic synergy may reflect an interaction between the intra-S-phase and G_2/M checkpoint defects ensuing from Mre11 complex hypomorphism and the NHEJ defects associated with the *Prkdc*$^{scid/scid}$ genotype. Alternatively, synergy may result from the coincident reductions in DNA repair processes mediated by the Mre11 complex and DNA-PKcs. Given the cell cycle-restricted penetrance of the *Nbs1*$^{\Delta B/\Delta B}$ and *Mre11*$^{ATLD1/ATLD1}$ phenotypes, either scenario implicitly requires that DNA-PKcs influence the DNA damage response in S and G_2, in addition to fulfilling its role in G_1 cells.

We tested this interpretation using *Nbs1*$^{\Delta C/\Delta C}$ and *Smc1*$^{2SA/2SA}$ murine mutants, both of which exhibit defects in the intra-S-phase checkpoint but have functional G_2/M checkpoint responses (27, 47). In contrast to the *Nbs1*$^{\Delta B/\Delta B}$ and *Mre11*$^{ATLD1/ATLD1}$ mutations, the *Nbs1*$^{\Delta C/\Delta C}$ and *Prkdc*$^{scid/scid}$ mutations exhibited no synthetic genetic interaction in double-mutant mice; the expected number of double-mutant pups was obtained, and no developmental defects were evident (Fig. 1C). The Nbs1$^{\Delta C}$ protein lacks a C-terminal domain implicated in interaction between ATM and the Mre11 complex (47). This interaction promotes the phosphorylation of the cohesin subunit SMC1 by ATM, a modification that is required for the full imposition of the intra-S-phase checkpoint (27). Intercrosses between *Prkdc*^{scid} mice and mice expressing an allele of *SMC1* (*Smc1*^{2SA}), lacking ATM consensus phosphorylation sites, were similarly unaffected. *Smc1*$^{2SA/2SA}$ *Prkdc*$^{scid/scid}$ mice were born at the expected ratios and did not exhibit any overt developmental defects, with the exception of the immunodeficiency characteristic of *Prkdc*$^{scid/scid}$ mice (Fig. 1C and data not shown).

DNA-PKcs regulates the Artemis nuclease, which is required for hairpin opening during V(D)J recombination, as well as the repair of some IR-induced lesions (20, 33, 39, 41). ATM and the Mre11 complex have also been suggested previously to regulate Artemis in response to IR (39). Thus, a second potential mechanism for the observed synergy may be the additive effects of Mre11 complex hypomorphism and impaired NHEJ associated with the misregulation of the Artemis nuclease. If so, then Artemis deficiency in the context of Mre11 complex hypomorphism (i.e., in *Nbs1*$^{\Delta B/\Delta B}$ or *Prkdc*$^{scid/scid}$ mice) might produce a phenocopy of the *Nbs1*$^{\Delta B/\Delta B}$ *Prkdc*$^{scid/scid}$ phenotype. To test this, *Nbs1*$^{\Delta B/\Delta B}$ *Art*$^{-/-}$ and *Prkdc*$^{scid/scid}$ *Art*$^{-/-}$ mice were generated. Both *Nbs1*$^{\Delta B/\Delta B}$ *Art*$^{-/-}$ and *Art*$^{-/-}$ *Prkdc*$^{scid/scid}$ double-mutant mice were born at the expected ratios, without any overt phenotypic synergy (Fig. 1C).

Together, these data indicate that an Artemis-independent function of DNA-PKcs is required for the viability of mutants with defects in DNA damage responses in the S and G_2 phases of the cell cycle. That the phenotypes of *Nbs1*$^{\Delta B/\Delta B}$ mice are mild relative to those of *Atm*$^{-/-}$ and *Mre11*$^{ATLD1/ATLD1}$ mice may account for the partial (as opposed to complete) lethality of the *Nbs1*$^{\Delta B/\Delta B}$ *Prkdc*$^{scid/scid}$ genotype.

Defects in cellular growth and chromosomal stability. The synergy between the *Nbs1*$^{\Delta B}$ and *Prkdc*^{scid} alleles was evident at the level of cell growth, chromosomal instability, and sensitivity to IR in cell cultures from *Nbs1*$^{\Delta B/\Delta B}$ *Prkdc*$^{scid/scid}$ mouse specimens. *Nbs1*$^{\Delta B/\Delta B}$ *Prkdc*$^{scid/scid}$ MEFs exhibited a marked growth defect compared to either wild-type (WT) or single-mutant cultures (Fig. 2A). WT and *Prkdc*$^{scid/scid}$ MEFs displayed similar growth characteristics, whereas *Nbs1*$^{\Delta B/\Delta B}$ MEFs showed a slight reduction in proliferation (Fig. 2A). By p3, *Nbs1*$^{\Delta B/\Delta B}$ *Prkdc*$^{scid/scid}$ MEFs showed high levels of senescence-associated β-galactosidase (SA-β-Gal) activity compared to those of either single mutant, indicating that the growth defect was the result of premature senescence (Fig. 2B).

Nbs1$^{\Delta B/\Delta B}$ *Prkdc*$^{scid/scid}$ EFs and MEFs showed increased sensitivity to IR compared to WT or single-mutant cell cultures (Fig. 2C and data not shown). In contrast, *Nbs1*$^{\Delta B/\Delta B}$ *Prkdc*$^{scid/scid}$ MEFs were not more sensitive than *Nbs1*$^{\Delta B/\Delta B}$ MEFs to agents such as CPT and MMC that induce breaks specifically during S phase (Fig. 2D and E).

As cell cultures from *Nbs1*$^{\Delta B/\Delta B}$ *Prkdc*$^{scid/scid}$ embryos and ears were highly sensitive to IR and exhibited severe growth defects, we analyzed genomic stability in cell cultures derived from single and double mutants. Early-passage *Nbs1*$^{\Delta B/\Delta B}$ *Prkdc*$^{scid/scid}$ MEF cultures exhibited higher frequencies of chromosome bridges and micronuclei than any of the other lines tested (Fig. 3A); WT, *Nbs1*$^{\Delta B/\Delta B}$, and *Prkdc*$^{scid/scid}$ MEFs each displayed low percentages of mitotic aberrations (Fig. 3A).

To further characterize the nature of the genomic instability, we analyzed aberrations in metaphase chromosome spreads of early-passage EF and MEF cultures. Chromosomal aberrations were evident in less than 20% of cells in WT, *Nbs1*$^{\Delta B/\Delta B}$, and *Prkdc*$^{scid/scid}$ MEF and EF cultures, whereas more than 35 to 50% of *Nbs1*$^{\Delta B/\Delta B}$ *Prkdc*$^{scid/scid}$ cells exhibited spontaneous aberrations that were commonly manifested as chromatid breaks (Fig. 3B; see also Fig. S1 in the supplemental material), indicating that they arose during or after S phase.

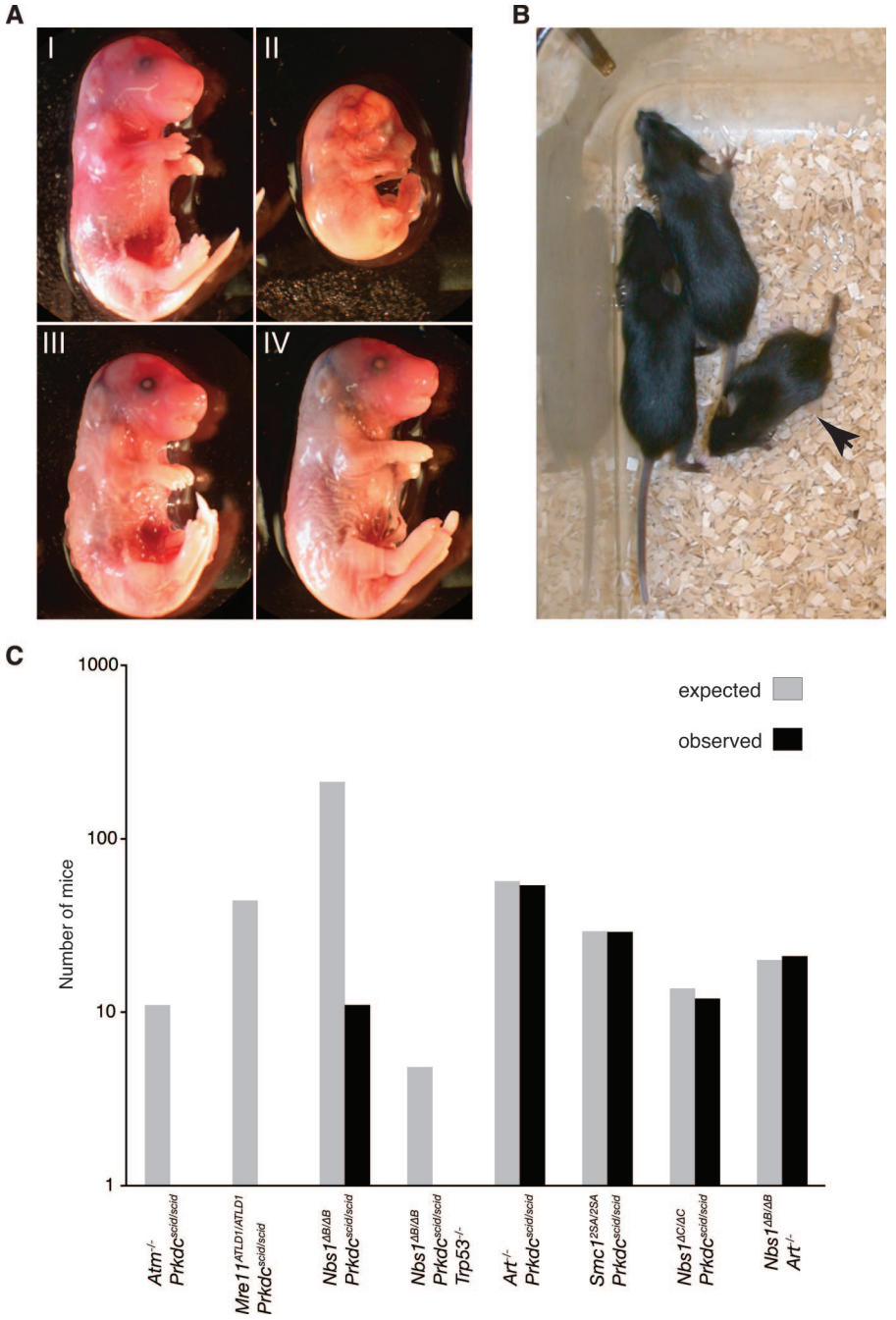

FIG. 1. Genetic interactions with the *Prkdc*^{scid} allele. (A) Embryos isolated from *Nbs1*$^{+/\Delta B}$ *Prkdc*$^{scid/scid}$ breedings at E15.5. (I) *Nbs1*$^{+/+}$ *Prkdc*$^{scid/scid}$ embryo. (II) *Nbs1*$^{\Delta B/\Delta B}$ *Prkdc*$^{scid/scid}$ embryo. (III and IV) *Nbs1*$^{+/\Delta B}$ *Prkdc*$^{scid/scid}$ embryos. (B) Female *Nbs1*$^{\Delta B/\Delta B}$ *Prkdc*$^{scid/scid}$ pup (arrow) with *Nbs1*$^{+/\Delta B}$ *Prkdc*$^{scid/scid}$ littermates at 1 month of age. All double mutants were runted, and 10 of 11 had a short, rigid, kinked tail. (C) Synthetic lethality was observed in *Atm*$^{-/-}$ *Prkdc*$^{scid/scid}$ and *Mre11*$^{ATLD1/ATLD1}$ *Prkdc*$^{scid/scid}$ embryos. Partial synthetic lethality of the *Nbs1*$^{\Delta B}$ and *Prkdc*^{scid} alleles was observed, while *Nbs1*$^{\Delta B/\Delta B}$ *Art*$^{-/-}$, *Smc1*$^{2SA/2SA}$ *Prkdc*$^{scid/scid}$, *Nbs1*$^{\Delta C/\Delta C}$ *Prkdc*$^{scid/scid}$, and *Art*$^{-/-}$ *Prkdc*$^{scid/scid}$ double mutants were born at expected ratios. The loss of p53 did not eliminate the synthetic lethality of the *Nbs1*$^{\Delta B/\Delta B}$ *Prkdc*$^{scid/scid}$ genotype.

Defects in cell growth, enhanced IR sensitivity, and increased chromosomal instability in *Nbs1*$^{\Delta B/\Delta B}$ *Prkdc*$^{scid/scid}$ cultures were not due to the loss of Artemis function, as *Nbs1*$^{\Delta B/\Delta B}$ *Art*$^{-/-}$ and single-mutant cell cultures grew at similar rates (see Fig. S2 in the supplemental material) and *Nbs1*$^{\Delta B/\Delta B}$ *Art*$^{-/-}$ cultures did not display increased chromosomal aberrations or IR sensitivity compared to single-mutant cultures (Fig. 3B; see Fig. S3 in the supplemental material) compared to WT cell cultures. These data indicate that DNA-PKcs plays an Artemis-independent role in the maintenance of chromosomal stability that is crucial in the context of impaired S- and G_2-phase DSB signaling.

Influence of Nbs1 hypomorphism and DNA-PKcs deficiency on NHEJ. Both the Mre11 complex and DNA-PK have been implicated in the NHEJ pathway of DSB repair. A potential

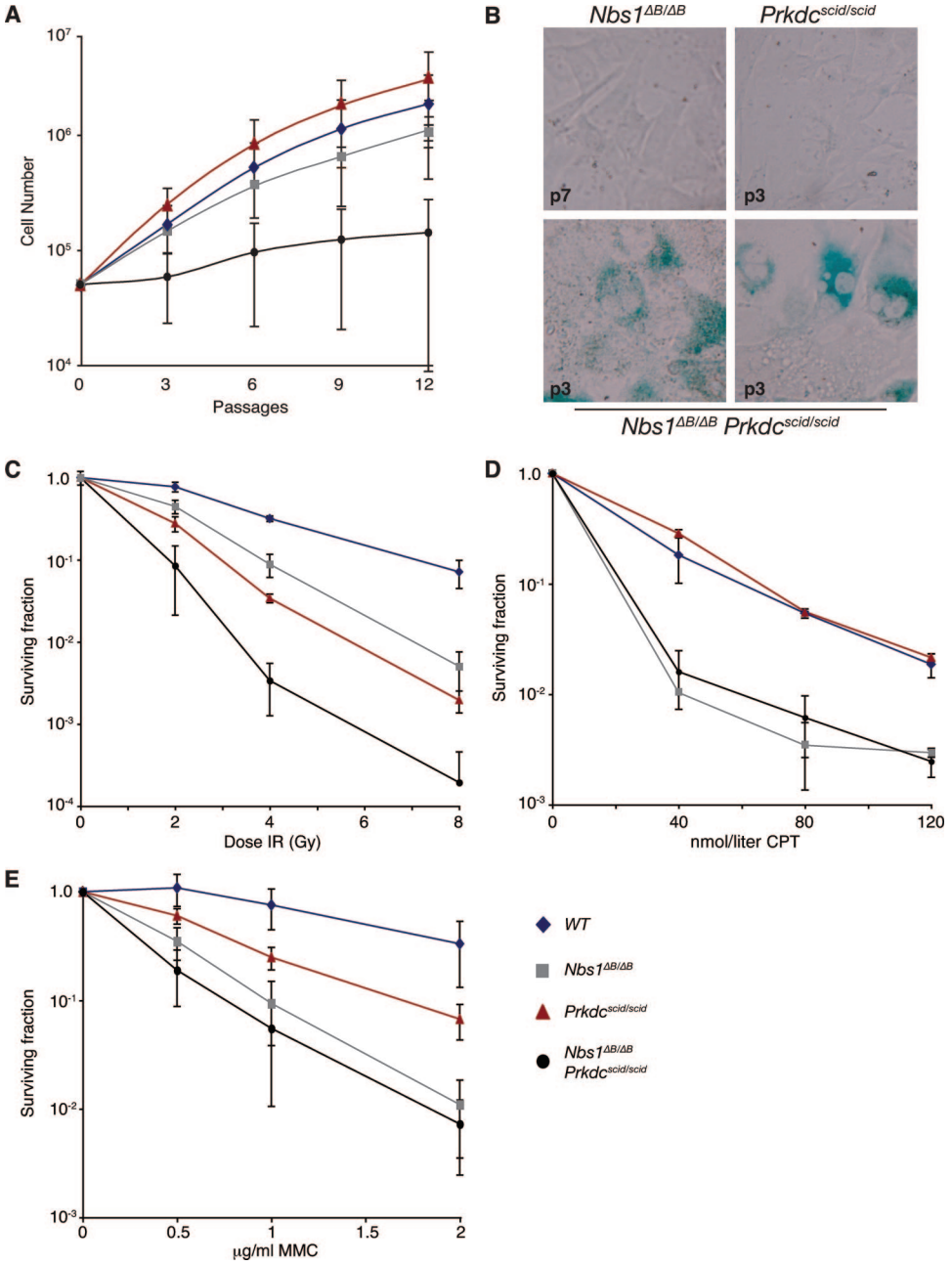

FIG. 2. Analysis of cell growth and survival. (A) The cell growth of primary MEFs of the indicated genotypes was analyzed using a modified 3T3 protocol. *Nbs1*$^{\Delta B/\Delta B}$ *Prkdc*$^{scid/scid}$ cell cultures showed little proliferation compared to WT, *Prkdc*$^{scid/scid}$, or *Nbs1*$^{\Delta B/\Delta B}$ cell cultures. (B) Early-passage MEFs were stained for SA-β-Gal activity. p3 *Nbs1*$^{\Delta B/\Delta B}$ *Prkdc*$^{scid/scid}$ cultures showed increased SA-β-Gal activity compared to p3 *Prkdc*$^{scid/scid}$ or p7 *Nbs1*$^{\Delta B/\Delta B}$ MEFs, where little activity is detectable. (C) SV40-transformed EFs of the indicated genotypes were exposed to IR and assessed for colony formation. *Nbs1*$^{\Delta B/\Delta B}$ *Prkdc*$^{scid/scid}$ EFs were acutely sensitive to IR-induced damage, and this sensitivity was also observed in MEF cultures (data not shown). Enhanced sensitivity in *Nbs1*$^{\Delta B/\Delta B}$ *Art*$^{-/-}$ cell cultures was not observed (see Fig. S3 in the supplemental material). (D and E) SV40-transformed MEFs were exposed to the indicated doses of CPT for 24 h (D) or to the DNA cross-linker MMC for 2 h (E), and survival was assessed by monitoring colony formation. Double-mutant *Nbs1*$^{\Delta B/\Delta B}$ *Prkdc*$^{scid/scid}$ MEFs did not display increased sensitivity to either agent compared to that of single-mutant *Nbs1*$^{\Delta B/\Delta B}$ MEFs.

explanation for the phenotypic synergy we observed between the *Prkdc*^{scid} and *Nbs1*$^{\Delta B}$ alleles was that NHEJ was more severely affected in *Nbs1*$^{\Delta B/\Delta B}$ *Prkdc*$^{scid/scid}$ double mutants than in single mutants. To address this possibility, we analyzed the end joining of fragments created by restriction enzyme- or *RAG*-induced breaks in plasmid substrates. WT, *Nbs1*$^{\Delta B/\Delta B}$, *Prkdc*$^{scid/scid}$, and *Nbs1*$^{\Delta B/\Delta B}$ *Prkdc*$^{scid/scid}$ cell cultures (see Fig. S4 in the supplemental material) were able to repair complementary or noncomplementary ends generated by restriction enzymes, and no reduction in the fidelity of joining was observed in any case (see Table S2 in the supplemental material). *Nbs1*$^{\Delta B/\Delta B}$ *Prkdc*$^{scid/scid}$ cells also retained the ability to rejoin

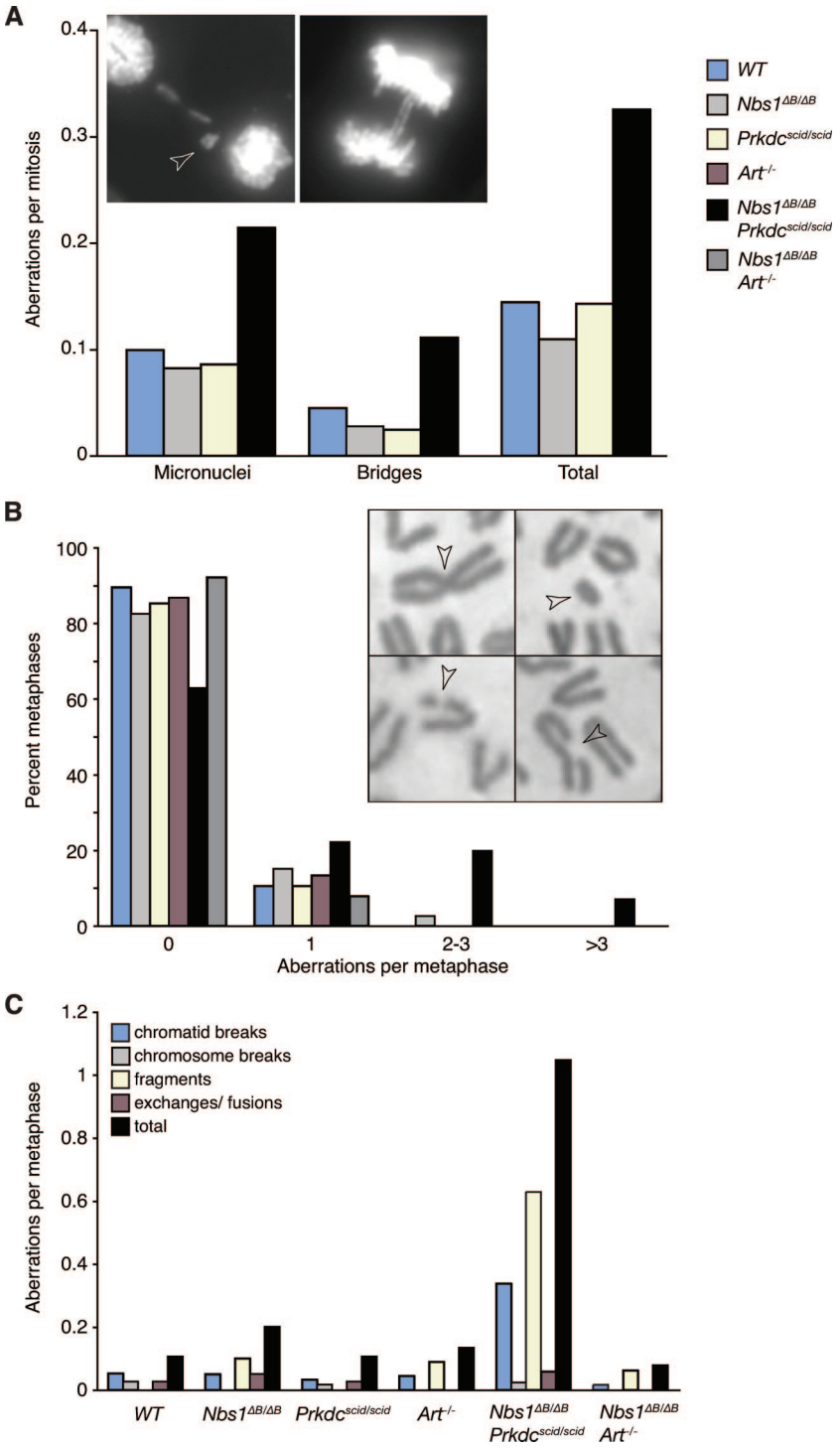

FIG. 3. Genomic instability in fibroblast cultures. (A) Increased mitotic aberrations in DAPI-stained *Nbs1*$^{\Delta B/\Delta B}$ *Prkdc*$^{scid/scid}$ MEFs were observed. Examples of the aberrations scored, the micronucleus (left; arrowhead) and chromosome bridges (right), are shown. (B) Metaphase aberrations in early-passage (p3 to p5) EFs of the indicated genotypes were scored. *Nbs1*$^{\Delta B/\Delta B}$ *Prkdc*$^{scid/scid}$ double mutants showed increased spontaneous aberrations compared to other mutants, which were indistinguishable from the WT. Examples of a chromosome fusion (top left), a chromosome fragment (top right), and two chromatid breaks (bottom left and right) are shown and are indicated by arrowheads. (C) Aberrations in *Nbs1*$^{\Delta B/\Delta B}$ *Prkdc*$^{scid/scid}$ cultures were primarily chromatid breaks and fragments. Similar results were obtained in analyses of MEF cultures (see Fig. S1 in the supplemental material).

fragments produced by *RAG* genes, as signal joints formed in *Nbs1*$^{\Delta B/\Delta B}$ *Prkdc*$^{scid/scid}$ cell cultures (L. Deriano, T. H. Stracker, A. Baker, J. H. J. Petrini, and D. B. Roth, submitted for publication).

Prkdc$^{scid/scid}$ and *Prkdc*$^{-/-}$ fibroblasts have been reported previously to exhibit spontaneous leading-strand-specific telomere fusions that become more evident when cells are immortalized (1, 2, 18, 21). As we did not observe increased fusions in early-passage (p2 to p3) *Prkdc*$^{scid/scid}$ MEF or EF cultures (Fig. 3C; see also Fig. S1 in the supplemental material), we assessed chromosomal aberrations in SV40-immortalized cultures by using telomere-specific FISH. Whereas neither WT nor *Nbs1*$^{\Delta B/\Delta B}$ cultures showed an increase in fusions, a strong increase in multiple *Prkdc*$^{scid/scid}$ cultures was observed, with most metaphases harboring one or two telomere fusions (i.e., fusions that contain a telomeric FISH signal) (Fig. 4A). This phenotype was not due to impaired Artemis activity, as increased fusions were not observed in multiple primary or transformed *Art*$^{-/-}$ cultures (Fig. 3C and data not shown).

Spontaneous fusions were observed more frequently in transformed *Nbs1*$^{\Delta B/\Delta B}$ *Prkdc*$^{scid/scid}$ cells than in WT or *Nbs1*$^{\Delta B/\Delta B}$ cells, but *Nbs1*$^{\Delta B/\Delta B}$ *Prkdc*$^{scid/scid}$ cultures showed a significant decrease in chromosome fusions compared to *Prkdc*$^{scid/scid}$ cultures (Fig. 4A and data not shown). To determine if the difference in the number of fusions we observed between *Prkdc*$^{scid/scid}$ and *Nbs1*$^{\Delta B/\Delta B}$ *Prkdc*$^{scid/scid}$ cell cultures reflected clonal events that had arisen prior to transformation, as opposed to an ongoing fusion process, we performed DAPI banding to identify the chromosomes involved. Chromosome fusions in *Prkdc*$^{scid/scid}$ cultures were nonclonal, indicating that chromosome breakage and rejoining were continually occurring in cultured cells (see Table S3 in the supplemental material).

We examined the ability of double-mutant cells to generate chromosome fusions by an alternative means. The expression of a dominant negative form of Trf2, Trf2$^{\Delta B\Delta M}$, compromises the shelterin complex that protects chromosome ends and results in chromosomal fusions dependent upon the NHEJ factors ligase 4 and Ku70 (7, 44). The expression of Trf2$^{\Delta B\Delta M}$ from an adenovirus vector resulted in chromosomal fusions in WT, *Nbs1*$^{\Delta B/\Delta B}$, *Prkdc*$^{scid/scid}$, and *Nbs1*$^{\Delta B/\Delta B}$ *Prkdc*$^{scid/scid}$ SV40-transformed cell cultures (Fig. 4B). Although increased numbers of fusions were observed in *Nbs1*$^{\Delta B/\Delta B}$ *Prkdc*$^{scid/scid}$ MEFs compared to those in WT and single-mutant cells, this increase is not likely to reflect an increased repair capacity of double-mutant cells. Rather, it more likely reflects the fact that *Nbs1*$^{\Delta B/\Delta B}$ *Prkdc*$^{scid/scid}$ cells were more permissive of transduction with adenovirus vectors than the other cell types, resulting in increased *Trf2*$^{\Delta B\Delta M}$ expression (Fig. 4C) and thereby increased numbers of uncapped telomeres. These data indicated that NHEJ functions required for the repair of nonhairpin-capped ends were largely intact in single-mutant or *Nbs1*$^{\Delta B/\Delta B}$ *Prkdc*$^{scid/scid}$ double-mutant backgrounds. The effect of the *Nbs1*$^{\Delta B}$ allele on spontaneous telomere fusions that arise in DNA-PKcs-deficient cells may suggest a subtle influence of the Mre11 complex hypomorphism on some aspects of NHEJ.

Cell cycle checkpoint regulation. We have shown previously that cells from both *Mre11*$^{ATLD1/ATLD1}$ and *Nbs1*$^{\Delta B/\Delta B}$ mutants exhibit intra-S-phase and G_2/M cell cycle defects (49, 52). Checkpoint deficiency was not seen in *Prkdc*$^{scid/scid}$ mice. In

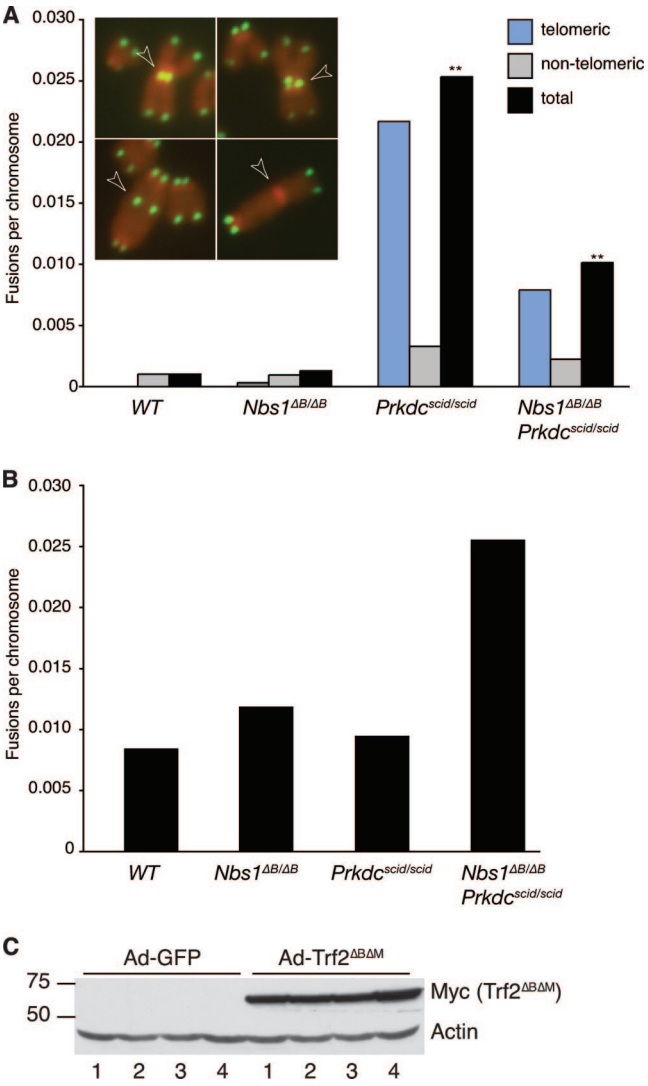

FIG. 4. (A) Analysis of spontaneous chromosome fusions in SV40-transformed cultures of the indicated genotypes by telomere-specific FISH. Examples of chromosome fusions with telomeric sequence (top left and bottom left), a chromatid fusion involving telomeric sequence (top right), and a chromosome fusion without telomeric sequence (bottom right) are shown and are indicated by arrowheads. The total fusions per chromosome are shown and are further classified as telomeric or nontelomeric. Increased spontaneous fusions involving telomere sequence were observed in transformed *Prkdc*$^{scid/scid}$ MEFs. Increased fusions in *Nbs1*$^{\Delta B/\Delta B}$ *Prkdc*$^{scid/scid}$ cultures were also observed, but their frequency was significantly reduced compared to that in *Prkdc*$^{scid/scid}$ single mutants (**, $P = 2.5e{-}9$; Wilcoxon rank sum test). DAPI banding data indicating that fusions were nonclonal are presented in Table S3 in the supplemental material. (B) Telomeric fusions induced by Trf2$^{\Delta B\Delta M}$ expression. Similar numbers of fusions were induced after Trf2$^{\Delta B\Delta M}$ expression regardless of the genotype. Fusion numbers were normalized to those in cultures infected with Ad-GFP to account for spontaneous fusion levels. (C) Western blot analysis of the expression of Myc-tagged Trf2$^{\Delta B\Delta M}$ in Ad-GFP- or Trf2$^{\Delta B\Delta M}$-expressing adenovirus (Ad-Trf2$^{\Delta B\Delta M}$)-infected MEFs. Lanes: 1, WT; 2, *Nbs1*$^{\Delta B/\Delta B}$; 3, *Prkdc*$^{scid/scid}$; and 4, *Nbs1*$^{\Delta B/\Delta B}$ *Prkdc*$^{scid/scid}$. Actin was included as a control for protein loading.

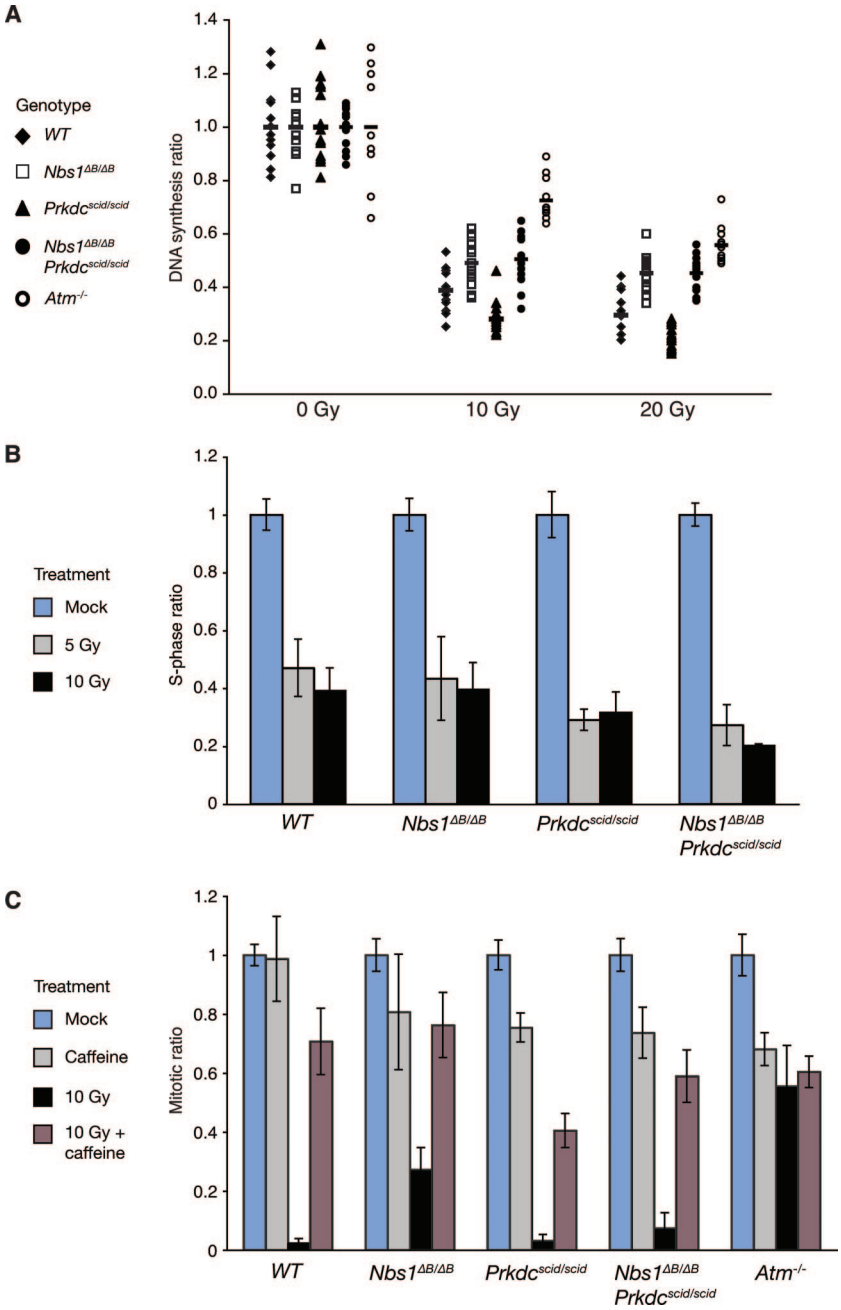

FIG. 5. Influence of DNA-PKcs on checkpoint induction. (A) The intra-S-phase checkpoint defect of *Nbs1*$^{\Delta B/\Delta B}$ mutants was indistinguishable from that of *Nbs1*$^{\Delta B/\Delta B}$ *Prkdc*$^{scid/scid}$ double mutants. *Prkdc*$^{scid/scid}$ MEFs showed significantly stronger arrest than WT MEFs (Wilcoxon rank sum test; at 10 Gy, $P = 3.18e{-}2$ [two sided], and at 20 Gy, $P = 2.98e{-}5$ [two sided]). *Atm*$^{-/-}$ cultures are shown for comparison. (B) G_1/S checkpoint responses in early-passage MEFs. Cultures were irradiated with 5 or 10 Gy, and DNA synthesis levels were normalized to those in untreated cultures. Both *Prkdc*$^{scid/scid}$ and *Nbs1*$^{\Delta B/\Delta B}$ *Prkdc*$^{scid/scid}$ MEFs showed stronger G_1/S checkpoint arrest than WT MEFs. Representative flow cytometry data are included in Fig. S5 in the supplemental material. (C) Deficient G_2/M checkpoint arrest in *Nbs1*$^{\Delta B/\Delta B}$ mutants was rescued by the *Prkdc*$^{scid/scid}$ mutation. MEFs of the indicated genotypes were mock treated, incubated with 10 mM caffeine, exposed to 10 Gy of IR, or exposed to 10 Gy IR and treated with 10 mM caffeine, and their mitotic indices were determined 1 h posttreatment. Treatment with caffeine abolished the checkpoint response in all backgrounds. Representative flow cytometry data are included in Fig. S6 in the supplemental material.

fact, DNA-PKcs deficiency led to a more robust intra-S-phase checkpoint arrest than that in WT cells, as *Prkdc*$^{scid/scid}$ MEFs showed a 79% reduction in DNA synthesis after treatment with 20 Gy, compared to the 70% reduction in DNA synthesis in WT MEFs. The defective intra-S-phase checkpoint responses characteristic of *Nbs1*$^{\Delta B/\Delta B}$ or *Smc1*$^{2SA/2SA}$ cell cultures were not influenced by the *Prkdc*^{scid} allele in *Nbs1*$^{\Delta B/\Delta B}$ *Prkdc*$^{scid/scid}$ (Fig. 5A) or *Smc1*$^{2SA/2SA}$ *Prkdc*$^{scid/scid}$ (data not shown) MEFs, indicating that enhanced S-phase arrest in *Prkdc*$^{scid/scid}$ MEFs is dependent upon Nbs1 and SMC1. As

both Nbs1 and SMC1 are regulated by ATM during the imposition of this checkpoint, these data imply that DNA-PKcs may antagonize ATM enforcement of the intra-S-phase checkpoint.

Similar to the intra-S-phase checkpoint responses we observed, a more robust G_1/S checkpoint response than WT has been reported in *Prkdc*$^{scid/scid}$ and *Prkdc*$^{-/-}$ MEFs (25). Early-passage *Nbs1*$^{\Delta B/\Delta B}$ MEF cultures exhibited normal G_1/S-phase checkpoint arrest, showing a 57% reduction in bromodeoxyuridine (BrdU)-positive cells following exposure to 5 Gy of IR, comparable to the 54% reduction in BrdU-positive cells in WT cultures. The checkpoint responses in both *Prkdc*$^{scid/scid}$ and *Nbs1*$^{\Delta B/\Delta B}$ *Prkdc*$^{scid/scid}$ cultures were more pronounced than those in WT and *Nbs1*$^{\Delta B/\Delta B}$ cultures (Fig. 5B; see also Fig. S5 in the supplemental material), as these cultures showed 71 and 73% reductions in BrdU-positive cells, respectively, after IR exposure.

The G_2/M checkpoint is dependent upon ATM and was defective in *Nbs1*$^{\Delta B/\Delta B}$ MEFs (Fig. 5C) (52, 55), whereas the G_2/M checkpoint in WT and *Prkdc*$^{scid/scid}$ cells was normal. DNA-PKcs deficiency abolished the G_2/M defect conferred by the *Nbs1*$^{\Delta B}$ allele; *Nbs1*$^{\Delta B/\Delta B}$ *Prkdc*$^{scid/scid}$ MEFs and WT MEFs arrested to similar degrees (Fig. 5C; see also Fig. S6 in the supplemental material). Checkpoint arrest in *Nbs1*$^{\Delta B/\Delta B}$ *Prkdc*$^{scid/scid}$ cells correlated with a decrease in the activity of cyclin B-associated kinase activity (see Fig. S7 in the supplemental material). The initiation of G_2/M checkpoint arrest is controlled by the activation of the ATM/ATR kinases, and the treatment of cells with checkpoint inhibitors, such as caffeine, blocks G_2/M arrest. To determine whether checkpoint activation in *Nbs1*$^{\Delta B/\Delta B}$ *Prkdc*$^{scid/scid}$ MEFs was still responsive to caffeine, we treated cells with 10 mM caffeine to block ATM/ATR activity (Fig. 5C). In all cases, checkpoint induction was impaired, suggesting that the elimination of the *Nbs1*$^{\Delta B/\Delta B}$ defect by the *Prkdc*$^{scid/scid}$ mutation was due to enhanced signaling through caffeine-sensitive ATM/ATR pathways. These data suggest that DNA-PKcs exerts an inhibitory effect on the DNA damage response in S and G_2, such that ATM and ATR-dependent checkpoint functions are more robust in DNA-PKcs-deficient cells than in WT cells.

DISCUSSION

The ATM arm of the DNA damage response influences recombinational DNA repair, DNA damage-dependent checkpoints, and apoptosis. Despite these broad influences, ATM is dispensable for organism and cell viability. However, ATM functions become essential for survival in the context of DNA-PKcs deficiency. In this study, we examined the mechanistic basis of this genetic interaction in *Prkdc*$^{scid/scid}$ mice. Mice expressing hypomorphic *Mre11*^{ATLD1} and *Nbs1*$^{\Delta B}$ alleles, which partially phenocopy the *Atm*$^{-/-}$ phenotype, were used as proxies for animals with ATM deficiency. The *Mre11*^{ATLD1} and *Nbs1*$^{\Delta B}$ alleles attenuate the intra-S-phase and G_2/M checkpoints and are associated with various degrees of impaired ATM activity, the *Nbs1*$^{\Delta B}$ phenotype being less severe than the *Mre11*^{ATLD1} phenotype (48).

Like *Atm*$^{-/-}$ *Prkdc*$^{scid/scid}$ mice, *Mre11*$^{ATLD1/ATLD1}$ *Prkdc*$^{scid/scid}$ embryos were nonviable (Table 1). However, viable *Nbs1*$^{\Delta B/\Delta B}$ *Prkdc*$^{scid/scid}$ pups were recovered at roughly 5% of the predicted Mendelian ratio. Consistent with this reduction in embryonic viability, *Nbs1*$^{\Delta B/\Delta B}$ *Prkdc*$^{scid/scid}$ mice exhibited severe defects. The cellular phenotypes were similarly severe, with double-mutant MEFs exhibiting premature senescence accompanied by extensive chromatid instability, anaphase bridges, micronuclei, and hypersensitivity to γ-irradiation.

Genetic analysis. The results of intercrosses between mice expressing the *Prkdc*^{scid} and *Smc1*^{2SA} (Fig. 1C), *Nbs1*$^{\Delta C}$ (Fig. 1C), or *Chk2* null (46) alleles suggested that deficiencies in the intra-S-phase checkpoint and apoptosis are not major contributors to the synthetic lethality. It remains possible that the G_2/M checkpoint or repair defects of the *Nbs1*$^{\Delta B}$ phenotype or some combination of phenotypes underlies the severe genetic interaction with the *Prkdc*^{scid} mutation.

Biochemical and genetic evidence suggests that the regulation of Artemis endonuclease activity is dependent on DNA-PKcs (20, 33, 41). The loss of Artemis in *Nbs1*$^{\Delta B/\Delta B}$ cell cultures did not cause increased sensitivity to IR (see Fig. S3 in the supplemental material), chromosomal aberrations (Fig. 3B), or cell growth defects (see Fig. S2 in the supplemental material). The birth of *Art*$^{-/-}$ *Nbs1*$^{\Delta B/\Delta B}$ and *Atm*$^{-/-}$ *Art*$^{-/-}$ mice at expected Mendelian ratios (Fig. 1C) (40) indicates that impaired Artemis function does not underlie the severe genetic interaction between DNA-PKcs and Mre11 complex hypomorphism (or ATM deficiency). This outcome also indicates that functions of DNA-PKcs in chromosome metabolism are not limited to Artemis regulation.

DSB repair and embryonic lethality. The loss of *Atm* or *Trp53* in a *Lig4* or *XRCC4* null background abolishes late embryonic lethality and neuronal apoptosis (15, 31, 42). The lack of synthetic lethality in *Atm*$^{-/-}$ *Lig4*$^{-/-}$ double mutants and the inability of p53 deficiency to rescue *Atm*$^{-/-}$ *Prkdc*$^{scid/scid}$ or *Nbs1*$^{\Delta B/\Delta B}$ *Prkdc*$^{scid/scid}$ embryos (Fig. 1C) indicate that deficient NHEJ is unlikely to underlie the severe genetic interaction between impaired ATM signaling and DNA-PKcs deficiency (19). Consistent with this, developmental analysis of *Atm*$^{-/-}$ *Prkdc*$^{scid/scid}$ and *Lig4*$^{-/-}$ embryos indicates that patterns of cell death in these backgrounds are temporally and mechanistically distinct (15, 19, 31).

Mice with a p53 null background that are doubly deficient in the homologous recombination (HR) factor Rad54 and either ligase IV or the DNA-PK holoenzyme component Ku80 are viable (9, 37). Similar to *Nbs1*$^{\Delta B/\Delta B}$ *Prkdc*$^{scid/scid}$ mice, these animals are born at a reduced frequency, are severely runted, and show increased IR sensitivity and high levels of chromatid breakage. As the Mre11 complex is involved in HR-mediated DSB repair, another explanation for the synthetic phenotype of *Nbs1*$^{\Delta B/\Delta B}$ *Prkdc*$^{scid/scid}$ mutants is the simultaneous impairment of HR and NHEJ. The inability of p53 deficiency to influence the survival of *Nbs1*$^{\Delta B/\Delta B}$ *Prkdc*$^{scid/scid}$ or *Atm*$^{-/-}$ *Prkdc*$^{scid/scid}$ animals, as well as the absence of increased chromosome breaks, which are observed in *Rad54*$^{-/-}$ *Lig4*$^{-/-}$ mice, makes this explanation unlikely (19, 37). This view is supported by the fact that embryonic lethality and severe cellular phenotypes were not observed previously in *Rad54*$^{-/-}$ *Prkdc*$^{scid/scid}$ mice or cell cultures (13). However, it is likely that the repair deficiencies of the *Nbs1*$^{\Delta B/\Delta B}$ phenotype are more severe than those of the *Rad54*$^{-/-}$ phenotype. The loss of Rad54 confers a mild HR defect on embryonic stem cells but not on MEFs, and *Rad54*$^{-/-}$ MEFs are not sensitive to IR

(13). In contrast, *Nbs1*$^{\Delta B/\Delta B}$ MEFs are highly sensitive to IR and CPT, due potentially to checkpoint defects or problems in the HR process itself, in which the Mre11 complex plays important roles in end resection and molecular bridging (48, 52). It is therefore possible that DNA-PKcs-deficient cells can tolerate a certain level of HR deficiency that is exceeded by the hypomorphic Nbs1 mutation.

Influence of DNA-PKcs on checkpoint regulation. The elimination of *Nbs1*$^{\Delta B}$ checkpoint deficiency in G_2/M, as well as the more robust induction of the G_1/S and intra-S-phase checkpoints, in *Prkdc*$^{scid/scid}$ cell cultures suggests that DNA-PKcs negatively influences ATM/ATR-mediated checkpoint induction throughout the cell cycle. Both the S-phase and G_2/M checkpoints in all genetic backgrounds were inhibited by caffeine, indicating that G_2/M checkpoint initiation in *Nbs1*$^{\Delta B/\Delta B}$ *Prkdc*$^{scid/scid}$ cultures was dependent upon ATM/ATR pathways that would normally be inhibited by DNA-PKcs. To a large extent, the novel checkpoint functions of DNA-PKcs elucidated here would not have been evident in other studies: inquiries regarding the checkpoint role of DNA-PKcs were designed to assess a positive role in checkpoint activation rather than an inhibitory one.

In this regard, it is important to note that DNA repair per se can be viewed as an inhibitor of checkpoint induction; hence, the phenotypic synergy observed with the *Nbs1*$^{\Delta B/\Delta B}$ mutation may indicate that the DNA repair functions of DNA-PKcs are manifested in S-phase cells. Certain results make this possibility unappealing. For example, *Prkdc*$^{scid/scid}$ cells are not sensitive to S-phase-specific damaging agents such as CPT (Fig. 2D), nor do *Nbs1*$^{\Delta B/\Delta B}$ *Prkdc*$^{scid/scid}$ cells exhibit greater sensitivity than *Nbs1*$^{\Delta B/\Delta B}$ cells. Similarly, the end joining of uncapped telomeres or DSB fragments generated by restriction enzymes is not further impaired in *Nbs1*$^{\Delta B/\Delta B}$ *Prkdc*$^{scid/scid}$ cultures (Fig. 4B; see Fig. S4 and Table S2 in the supplemental material). If the rescue of the *Nbs1*$^{\Delta B/\Delta B}$ G_2/M checkpoint by the *Prkdc*$^{scid/scid}$ mutation was attributable to impaired DSB repair associated with DNA-PKcs deficiency, subjecting *Nbs1*$^{\Delta B/\Delta B}$ cells to higher numbers of DSBs should produce a phenocopy of the double-mutant phenotype. No elimination of the *Nbs1*$^{\Delta B/\Delta B}$ checkpoint defects was evident at IR doses as high as 40 Gy (data not shown). Together, these data provide evidence for an unexpected role for DNA-PKcs in modulating ATM/ATR checkpoint signaling during S and G_2.

Artemis- and NHEJ-independent role for DNA-PKcs in chromosomal stability. The cellular functions of DNA-PKcs, the in vivo targets of its kinase activity, and the extent of its role in DNA repair remain largely unclear. The phenotypes of DNA-PKcs-deficient cell lines and animals are inconsistent with its playing an essential role in the end joining of fragments from clean DSBs, and DNA-PKcs-deficient cells show IR sensitivity that is intermediate between that of sensitive Lig4-deficient cells and that of mildly sensitive Artemis-deficient lines (39). Studies using DT40 knockout lines demonstrated that the IR sensitivity of DNA-PKcs null cell lines is highest in G_1 and early S phases, suggesting a link between IR sensitivity and G_1 repair deficiency (16). Concurrently, the levels of DNA-PKcs kinase activity and autophosphorylation, which is required for IR resistance, are high in G_1 and low in S phase (8, 30). Finally, the loss of DNA-PKcs in embryonic stem cells, which cycle between S and M and rely primarily on HR, does not result in radiosensitivity (17).

Considering that the major functions of DNA-PKcs in radioresistance, Artemis regulation, and NHEJ-mediated repair are restricted largely to G_1, the severe impact that DNA-PKcs deficiency had on embryonic development and chromosomal stability in the presence of hypomorphic Mre11 complex alleles was unexpected. Our data suggest that DNA-PKcs plays a regulatory role in maintaining chromosomal stability in S/G_2 phase when ATM-Mre11 complex signaling is compromised. Further, this function is independent of the previously described roles of DNA-PKcs in DSB repair.

Although the G_2/M damage response was enhanced in *Nbs1*$^{\Delta B/\Delta B}$ *Prkdc*$^{scid/scid}$ cell cultures compared to *Nbs1*$^{\Delta B/\Delta B}$ cell cultures, we observed increased levels of mitotic aberrations, such as chromosome bridges, as well as increased levels of spontaneous metaphase aberrations, including chromatid breaks and fragments, in *Nbs1*$^{\Delta B/\Delta B}$ *Prkdc*$^{scid/scid}$ cultures. These findings indicated that cells that escaped G_2 arrest and entered mitosis harbored extensive DNA damage. We propose that DNA-PKcs opposes the functions of ATM/ATR in the regulation of cell cycle progression through a direct or indirect influence on cyclin-dependent kinase activity. The simultaneous impairment of ATM signaling (directly or indirectly via Mre11 complex mutations) and DNA-PKcs function upsets this regulatory balance, leading to cytotoxic/static chromosomal damage and the attrition of cells through the activation of p53-independent senescence or cell death pathways in *Nbs1*$^{\Delta B/\Delta B}$ *Prkdc*$^{scid/scid}$ cells. Our results suggest that the simultaneous targeting of ATM-Mre11 complex and DNA-PKcs signaling pathways is highly cytotoxic, even in the absence of p53 function, and may represent a viable strategy for chemotherapeutic approaches.

ACKNOWLEDGMENTS

We thank Annalee Baker and Hussein Hussein for diligent maintenance of our animal colony; Titia de Lange, Andy Koff, and members of the Petrini and de Lange labs for helpful advice and discussions; and Rob Fisher and Claire Attwooll for critical reading of the manuscript.

T.H.S. was supported by an NIH National Research Service Award and is a Leukemia and Lymphoma Society special fellow, L.D. is a Leukemia and Lymphoma Society fellow, D.B.R. is supported by grants from the NIH, and J.H.J.P. is supported by NIH grants and the Jean and Joel Smilow Initiative.

REFERENCES

1. **Bailey, S. M., M. N. Cornforth, A. Kurimasa, D. J. Chen, and E. H. Goodwin.** 2001. Strand-specific postreplicative processing of mammalian telomeres. Science **293:**2462–2465.
2. **Bailey, S. M., J. Meyne, D. J. Chen, A. Kurimasa, G. C. Li, B. E. Lehnert, and E. H. Goodwin.** 1999. DNA double-strand break repair proteins are required to cap the ends of mammalian chromosomes. Proc. Natl. Acad. Sci. USA **96:**14899–14904.
3. **Bressan, D. A., B. K. Baxter, and J. H. Petrini.** 1999. The Mre11-Rad50-Xrs2 protein complex facilitates homologous recombination-based double-strand break repair in *Saccharomyces cerevisiae*. Mol. Cell. Biol. **19:**7681–7687.
4. **Buscemi, G., C. Savio, L. Zannini, F. Micciche, D. Masnada, M. Nakanishi, H. Tauchi, K. Komatsu, S. Mizutani, K. Khanna, P. Chen, P. Concannon, L. Chessa, and D. Delia.** 2001. Chk2 activation dependence on Nbs1 after DNA damage. Mol. Cell. Biol. **21:**5214–5222.
5. **Carney, J. P., R. S. Maser, H. Olivares, E. M. Davis, M. Le Beau, J. R. Yates III, L. Hays, W. F. Morgan, and J. H. Petrini.** 1998. The hMre11/hRad50 protein complex and Nijmegen breakage syndrome: linkage of double-strand break repair to the cellular DNA damage response. Cell **93:**477–486.
6. **Carson, C. T., R. A. Schwartz, T. H. Stracker, C. E. Lilley, D. V. Lee, and M. D. Weitzman.** 2003. The Mre11 complex is required for ATM activation and the G(2)/M checkpoint. EMBO J. **22:**6610–6620.
7. **Celli, G. B., E. L. Denchi, and T. de Lange.** 2006. Ku70 stimulates fusion of

dysfunctional telomeres yet protects chromosome ends from homologous recombination. Nat. Cell Biol. **8:**885–890.
8. **Chen, B. P., D. W. Chan, J. Kobayashi, S. Burma, A. Asaithamby, K. Morotomi-Yano, E. Botvinick, J. Qin, and D. J. Chen.** 2005. Cell cycle dependence of DNA-dependent protein kinase phosphorylation in response to DNA double strand breaks. J. Biol. Chem. **280:**14709–14715.
9. **Couedel, C., K. D. Mills, M. Barchi, L. Shen, A. Olshen, R. D. Johnson, A. Nussenzweig, J. Essers, R. Kanaar, G. C. Li, F. W. Alt, and M. Jasin.** 2004. Collaboration of homologous recombination and nonhomologous end-joining factors for the survival and integrity of mice and cells. Genes Dev. **18:**1293–1304.
10. **de Jager, M., J. van Noort, D. C. van Gent, C. Dekker, R. Kanaar, and C. Wyman.** 2001. Human Rad50/Mre11 is a flexible complex that can tether DNA ends. Mol. Cell **8:**1129–1135.
11. **Difilippantonio, S., A. Celeste, M. J. Kruhlak, Y. Lee, M. J. Difilippantonio, L. Feigenbaum, S. P. Jackson, P. J. McKinnon, and A. Nussenzweig.** 2007. Distinct domains in Nbs1 regulate irradiation-induced checkpoints and apoptosis. J. Exp. Med. **204:**1003–1011.
12. **Di Virgilio, M., and J. Gautier.** 2005. Repair of double-strand breaks by nonhomologous end joining in the absence of Mre11. J. Cell Biol. **171:**765–771.
13. **Essers, J., H. van Steeg, J. de Wit, S. M. Swagemakers, M. Vermeij, J. H. Hoeijmakers, and R. Kanaar.** 2000. Homologous and non-homologous recombination differentially affect DNA damage repair in mice. EMBO J. **19:**1703–1710.
14. **Falck, J., J. Coates, and S. P. Jackson.** 2005. Conserved modes of recruitment of ATM, ATR and DNA-PKcs to sites of DNA damage. Nature **434:**605–611.
15. **Frank, K. M., N. E. Sharpless, Y. Gao, J. M. Sekiguchi, D. O. Ferguson, C. Zhu, J. P. Manis, J. Horner, R. A. DePinho, and F. W. Alt.** 2000. DNA ligase IV deficiency in mice leads to defective neurogenesis and embryonic lethality via the p53 pathway. Mol. Cell **5:**993–1002.
16. **Fukushima, T., M. Takata, C. Morrison, R. Araki, A. Fujimori, M. Abe, K. Tatsumi, M. Jasin, P. K. Dhar, E. Sonoda, T. Chiba, and S. Takeda.** 2001. Genetic analysis of the DNA-dependent protein kinase reveals an inhibitory role of Ku in late S-G2 phase DNA double-strand break repair. J. Biol. Chem. **276:**44413–44418.
17. **Gao, Y., J. Chaudhuri, C. Zhu, L. Davidson, D. T. Weaver, and F. W. Alt.** 1998. A targeted DNA-PKcs-null mutation reveals DNA-PK-independent functions for KU in V(D)J recombination. Immunity **9:**367–376.
18. **Gilley, D., H. Tanaka, M. P. Hande, A. Kurimasa, G. C. Li, M. Oshimura, and D. J. Chen.** 2001. DNA-PKcs is critical for telomere capping. Proc. Natl. Acad. Sci. USA **98:**15084–15088.
19. **Gladdy, R. A., L. M. Nutter, T. Kunath, J. S. Danska, and C. J. Guidos.** 2006. p53-independent apoptosis disrupts early organogenesis in embryos lacking both ataxia-telangiectasia mutated and Prkdc. Mol. Cancer Res. **4:**311–318.
20. **Goodarzi, A. A., Y. Yu, E. Riballo, P. Douglas, S. A. Walker, R. Ye, C. Harer, C. Marchetti, N. Morrice, P. A. Jeggo, and S. P. Lees-Miller.** 2006. DNA-PK autophosphorylation facilitates Artemis endonuclease activity. EMBO J. **25:**3880–3889.
21. **Goytisolo, F. A., E. Samper, S. Edmonson, G. E. Taccioli, and M. A. Blasco.** 2001. The absence of the DNA-dependent protein kinase catalytic subunit in mice results in anaphase bridges and in increased telomeric fusions with normal telomere length and G-strand overhang. Mol. Cell. Biol. **21:**3642–3651.
22. **Gurley, K. E., and C. J. Kemp.** 2001. Synthetic lethality between mutation in Atm and DNA-PK(cs) during murine embryogenesis. Curr. Biol. **11:**191–194.
23. **Hopfner, K. P., L. Craig, G. Moncalian, R. A. Zinkel, T. Usui, B. A. Owen, A. Karcher, B. Henderson, J. L. Bodmer, C. T. McMurray, J. P. Carney, J. H. Petrini, and J. A. Tainer.** 2002. The Rad50 zinc-hook is a structure joining Mre11 complexes in DNA recombination and repair. Nature **418:**562–566.
24. **Ivanov, E. L., V. G. Korolev, and F. Fabre.** 1992. *XRS2*, a DNA repair gene of *Saccharomyces cerevisiae*, is needed for meiotic recombination. Genetics **132:**651–664.
25. **Jimenez, G. S., F. Bryntesson, M. I. Torres-Arzayus, A. Priestley, M. Beeche, S. Saito, K. Sakaguchi, E. Appella, P. A. Jeggo, G. E. Taccioli, G. M. Wahl, and M. Hubank.** 1999. DNA-dependent protein kinase is not required for the p53-dependent response to DNA damage. Nature **400:**81–83.
26. **Kim, S.-T., B. Xu, and M. B. Kastan.** 2002. Involvement of the cohesin protein Smc1, in Atm-dependent and independent responses to DNA damage. Genes Dev. **16:**560–570.
27. **Kitagawa, R., C. J. Bakkenist, P. J. McKinnon, and M. B. Kastan.** 2004. Phosphorylation of SMC1 is a critical downstream event in the ATM-NBS1-BRCA1 pathway. Genes Dev. **18:**1423–1438.
28. **Lansdorp, P. M., N. P. Verwoerd, F. M. van de Rijke, V. Dragowska, M. T. Little, R. W. Dirks, A. K. Raap, and H. J. Tanke.** 1996. Heterogeneity in telomere length of human chromosomes. Hum. Mol. Genet. **5:**685–691.
29. **Lee, J. H., and T. T. Paull.** 2007. Activation and regulation of ATM kinase activity in response to DNA double-strand breaks. Oncogene **26:**7741–7748.
30. **Lee, S. E., R. A. Mitchell, A. Chieng, and E. A. Hendrickson.** 1997. Evidence for DNA-PK-dependent and -independent DNA double-strand break repair pathways in mammalian cells as a function of the cell cycle. Mol. Cell. Biol. **17:**1425–1433.
31. **Lee, Y., D. E. Barnes, T. Lindahl, and P. J. McKinnon.** 2000. Defective neurogenesis resulting from DNA ligase IV deficiency requires Atm. Genes Dev. **14:**2576–2580.
32. **Lim, D. S., S. T. Kim, B. Xu, R. S. Maser, J. Lin, J. H. Petrini, and M. B. Kastan.** 2000. ATM phosphorylates p95/nbs1 in an S-phase checkpoint pathway. Nature **404:**613–617.
33. **Ma, Y., U. Pannicke, K. Schwarz, and M. R. Lieber.** 2002. Hairpin opening and overhang processing by an Artemis/DNA-dependent protein kinase complex in nonhomologous end joining and V(D)J recombination. Cell **108:**781–794.
34. **Manolis, K. G., E. R. Nimmo, E. Hartsuiker, A. M. Carr, P. A. Jeggo, and R. C. Allshire.** 2001. Novel functional requirements for non-homologous DNA end joining in Schizosaccharomyces pombe. EMBO J. **20:**210–221.
35. **Maser, R. S., O. K. Mirzoeva, J. Wells, H. Olivares, B. R. Williams, R. Zinkel, P. J. Farnham, and J. H. J. Petrini.** 2001. The MRE11 complex and DNA replication: linkage to E2F and sites of DNA synthesis. Mol. Cell. Biol. **21:**6006–6016.
36. **Matsuoka, S., B. A. Ballif, A. Smogorzewska, E. R. McDonald III, K. E. Hurov, J. Luo, C. E. Bakalarski, Z. Zhao, N. Solimini, Y. Lerenthal, Y. Shiloh, S. P. Gygi, and S. J. Elledge.** 2007. ATM and ATR substrate analysis reveals extensive protein networks responsive to DNA damage. Science **316:**1160–1166.
37. **Mills, K. D., D. O. Ferguson, J. Essers, M. Eckersdorff, R. Kanaar, and F. W. Alt.** 2004. Rad54 and DNA ligase IV cooperate to maintain mammalian chromatid stability. Genes Dev. **18:**1283–1292.
38. **Mirzoeva, O. K., and J. H. Petrini.** 2003. DNA replication-dependent nuclear dynamics of the Mre11 complex. Mol. Cancer Res. **1:**207–218.
39. **Riballo, E., M. Kuhne, N. Rief, A. Doherty, G. C. Smith, M. J. Recio, C. Reis, K. Dahm, A. Fricke, A. Krempler, A. R. Parker, S. P. Jackson, A. Gennery, P. A. Jeggo, and M. Lobrich.** 2004. A pathway of double-strand break rejoining dependent upon ATM, Artemis, and proteins locating to gamma-H2AX foci. Mol. Cell **16:**715–724.
40. **Rooney, S., F. W. Alt, J. Sekiguchi, and J. P. Manis.** 2005. Artemis-independent functions of DNA-dependent protein kinase in Ig heavy chain class switch recombination and development. Proc. Natl. Acad. Sci. USA **102:**2471–2475.
41. **Rooney, S., J. Sekiguchi, C. Zhu, H. L. Cheng, J. Manis, S. Whitlow, J. DeVido, D. Foy, J. Chaudhuri, D. Lombard, and F. W. Alt.** 2002. Leaky Scid phenotype associated with defective V(D)J coding end processing in Artemis-deficient mice. Mol. Cell **10:**1379–1390.
42. **Sekiguchi, J., D. O. Ferguson, H. T. Chen, E. M. Yang, J. Earle, K. Frank, S. Whitlow, Y. Gu, Y. Xu, A. Nussenzweig, and F. W. Alt.** 2001. Genetic interactions between ATM and the nonhomologous end-joining factors in genomic stability and development. Proc. Natl. Acad. Sci. USA **98:**3243–3248.
43. **Shiloh, Y.** 2003. ATM and related protein kinases: safeguarding genome integrity. Nat. Rev. Cancer **3:**155–168.
44. **Smogorzewska, A., J. Karlseder, H. Holtgreve-Grez, A. Jauch, and T. de Lange.** 2002. DNA ligase IV-dependent NHEJ of deprotected mammalian telomeres in G1 and G2. Curr. Biol. **12:**1635–1644.
45. **Stewart, G. S., R. S. Maser, T. Stankovic, D. A. Bressan, M. I. Kaplan, N. G. Jaspers, A. Raams, P. J. Byrd, J. H. Petrini, and A. M. Taylor.** 1999. The DNA double-strand break repair gene hMRE11 is mutated in individuals with an ataxia-telangiectasia-like disorder. Cell **99:**577–587.
46. **Stracker, T. H., S. S. Couto, C. Cordon-Cardo, T. Matos, and J. H. Petrini.** 2008. Chk2 suppresses the oncogenic potential of DNA replication-associated DNA damage. Mol. Cell **31:**21–32.
47. **Stracker, T. H., M. Morales, S. S. Couto, H. Hussein, and J. H. Petrini.** 2007. The carboxy terminus of NBS1 is required for induction of apoptosis by the MRE11 complex. Nature **447:**218–221.
48. **Stracker, T. H., J. W. Theunissen, M. Morales, and J. H. Petrini.** 2004. The Mre11 complex and the metabolism of chromosome breaks: the importance of communicating and holding things together. DNA Repair (Amsterdam) **3:**845–854.
49. **Theunissen, J. W., M. I. Kaplan, P. A. Hunt, B. R. Williams, D. O. Ferguson, F. W. Alt, and J. H. Petrini.** 2003. Checkpoint failure and chromosomal instability without lymphomagenesis in Mre11(ATLD1/ATLD1) mice. Mol. Cell **12:**1511–1523.
50. **Theunissen, J. W., and J. H. Petrini.** 2006. Methods for studying the cellular response to DNA damage: influence of the Mre11 complex on chromosome metabolism. Methods Enzymol. **409:**251–284.
51. **Uziel, T., Y. Lerenthal, L. Moyal, Y. Andegeko, L. Mittelman, and Y. Shiloh.** 2003. Requirement of the MRN complex for ATM activation by DNA damage. EMBO J. **22:**5612–5621.
52. **Williams, B. R., O. K. Mirzoeva, W. F. Morgan, J. Lin, W. Dunnick, and J. H. Petrini.** 2002. A murine model of Nijmegen breakage syndrome. Curr. Biol. **12:**648–653.
53. **Wiltzius, J. J., M. Hohl, J. C. Fleming, and J. H. Petrini.** 2005. The Rad50 hook domain is a critical determinant of Mre11 complex functions. Nat. Struct. Mol. Biol. **12:**403–407.

54. **Wu, X., V. Ranganathan, D. S. Weisman, W. F. Heine, D. N. Ciccone, T. B. O'Neill, K. E. Crick, K. A. Pierce, W. S. Lane, G. Rathbun, D. M. Livingston, and D. T. Weaver.** 2000. ATM phosphorylation of Nijmegen breakage syndrome protein is required in a DNA damage response. Nature **405:**477–482.
55. **Xu, B., S.-T. Kim, D.-S. Lim, and M. B. Kastan.** 2002. Two molecularly distinct G_2/M checkpoints are induced by ionizing irradiation. Mol. Cell. Biol. **22:**1049–1059.
56. **Yamaguchi-Iwai, Y., E. Sonoda, M. S. Sasaki, C. Morrison, T. Haraguchi, Y. Hiraoka, Y. M. Yamashita, T. Yagi, M. Takata, C. Price, N. Kakazu, and S. Takeda.** 1999. Mre11 is essential for the maintenance of chromosomal DNA in vertebrate cells. EMBO J. **18:**6619–6629.
57. **Yang, Y. G., A. Saidi, P. O. Frappart, W. Min, C. Barrucand, V. Dumon-Jones, J. Michelon, Z. Herceg, and Z. Q. Wang.** 2006. Conditional deletion of Nbs1 in murine cells reveals its role in branching repair pathways of DNA double-strand breaks. EMBO J. **25:**5527–5538.
58. **You, Z., C. Chahwan, J. Bailis, T. Hunter, and P. Russell.** 2005. ATM activation and its recruitment to damaged DNA require binding to the C terminus of Nbs1. Mol. Cell. Biol. **25:**5363–5379.